Available online www.jsaer.com

***Journal of Scientific and Engineering Research*, 2021, 8(12):129-136**

Research Article

ISSN: 2394-2630
CODEN(USA): JSERBR

Theoretical calculation of ^{13}C and ^{1}H NMR of 7-methoxy-1-tetralone thiosemicarbazone and 7-methoxy-1-tetralone 4-phenyl-3-thiosemicarbazone

GLINMA Bienvenu[1], KPOTIN Assongba Gaston*[2], AGNIMONHAN Finagnon Hyacinthe[1], GBAGUIDI Fernand[1], ATOHOUN Yacole Guy Sylvain[2]

[1]Laboratoire de Chimie Organique Physique et de Synthèse, Faculté des Sciences et Techniques, Université d'Abomey-Calavi, 02 BP 69 Bohicon, Benin,
[2]Laboratoire de Chimie Théorique et de Spectroscopie Moléculaire, Faculté des Sciences et Techniques, Université d'Abomey-Calavi, 03 BP 3409 Cotonou, Benin
Corresponding authors: gaston.kpotin@fast.uac.bj

Abstract In this work, we report the geometrical parameters and the ^{13}C and ^{1}H chemical shift of two thiosemicarbazones. The calculation are carried out by using DFT/6-31G(d,p) for the optimization of the geometrical parameters. The global reactivity indices are calculated for both molecule. For NMR calculation DFT method with 6-311G(d,p) and cc-PVTZ basis set and GIAO method are used. To take account the solvent the Polarizable Continuum Model (PCM) is used, but it not modify significantly the result obtained in gas phase. The results obtained are close with the experimental data. The ^{13}C NMR is best estimated than the ^{1}H NMR.

Keywords DFT, thiosemicarbazone, ^{13}C NMR, ^{1}H NMR, reactivity indices

1. Introduction

Schiff bases that contain an imino group (–RC=N–) are formed by the condensation of a primary amine with an active carbonyl group. A number of Schiff bases containing the imino functionality have been shown to have a wide range of biological activities, including antibacterial, antifungal, antidiabetic, antitumor, antiproliferative, anticancer, anticorrosive and anti-inflammatory activities [1,2]. It is believed that the biological activity is related to the hydrogen bonding through the imino group of Schiff bases with the active centers of the cell constituents [3]. Semicarbazones, thiosemicarbazones and their derivatives are the major subgroups of hydrazones (-C=N-N-) alongside thioaroylhydrazones and oxyaroylhydrazones. Thiosemicarbazones (TSCs) encompasses a class of compounds relevant in the pharmacological context. Their specific applicability varies in function of the appropriated chemical modification and their binding to different transition metals [4]. They have been studied for their antitumor, antiviral (including against HIV), antibacterial, antimalarial, antifungal, anti-inflammatory properties [5–10]. They were used in the analysis of metals for device applications relative to telecommunications, optical computing, optical storage and optical information processing [11]. The reasons for such pharmacological activities were due to the ability of thiosemicarbazones to chelate strongly with transition metal ions in biological systems binding through thio-ketosulphur and hydrazine nitrogen atoms. They represent validated drug leads that kill several species of protozoan parasites through the inhibition of cysteine proteases as well as other novel targets [12]. Their interest in medicinal chemistry has stimulated the development of new methods of preparing these molecules.

After the synthesis of the molecules, it is important to characterize then. The spectroscopy methods are useful for this target. The computational chemistry can predict some parameters as geometrical parameters [13,14], chemical shift [15–20], and reactivity indices [21–23]. There is several work using Density Functional Theory (DFT) method [24,25] to predict NMR data. In this work we use DFT method with functional B3LYP in different basis set. The aim of this work is to determine the correlation between the ^{13}C NMR and ^{1}H NMR calculated and the experimental data.

2. Computational details

The geometry of the molecules were fully optimized using the DFT and B3LYP functional [26], with different basis set 6-311G(d,p) and cc-PVTZ). The PCM model [27] (solvent DMSO-d6 and chloroform) was used to take into account the solvent effect on the equilibrium structures. Harmonic frequency calculations were carried out for geometries optimized to characterize the located stationary points on the potential energy surface as true minimum (all frequencies are real). Then, calculations of ^{1}H and ^{13}C magnetic shielding constants (σ), with chemical shifts (δ), obtained on a δ-scale relative to the TMS, taken as reference, were carried out using the Gauge-Independent Atomic Orbital (GIAO) method implemented by Wolinski et al. [28]. All calculations have been done with the Gaussian-09 package [29].

The molecules are

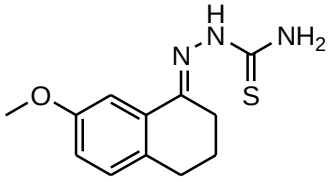

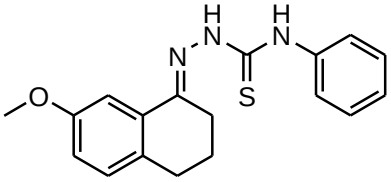

7-methoxy-1-tetralone thiosemicarbazone (**Mol 1**) 7-methoxy-1-tetralone 4-phenyl-3-thiosemicarbazone (**Mol 2**)

Figure 1: Structure of studies molecules

The reactivity indices are obtained by the following formula:

the chemical potential $\mu = (E_{HOMO} + E_{LUMO})/2$,

the hardness $\eta = E_{LUMO} - E_{HOMO}$,

the softness $\varsigma = 1/\eta$

the electrophilicity $\omega = \frac{\mu^2}{2\eta}$

3. Results and Discussion

3.1 Geometries and Reactivity Indices

Both molecules are optimized with 6-31G(d,p) basis set in DFT. There is no imaginary frequencies in the calculation of the vibration, the obtained geometries are the single point. The parameters are in table 1.

Table 1: Geometry parameters of molecules on DFT/6-31G(d,p) level

Mol1		Mol2	
	Length (Å)		Length (Å)
C^1C^2	1.39	C^1C^2	1.39
C^1C^6	1.40	C^1C^6	1.40
C^3C^7	1.49	C^3C^7	1.48
C^4C^8	1.51	C^4C^8	1.51
C^7N^{13}	1.29	C^7N^{13}	1.29
$N^{13}N^{14}$	1.42	$N^{13}N^{14}$	1.35
$N^{14}C^{15}$	1.37	$N^{14}C^{15}$	1.38

$C^{15}N^{16}$	1.36
$C^{15}S^{17}$	1.68
Angle (°)	
$C^{2}C^{1}O^{11}$	115.92
$C^{6}C^{1}O^{11}$	124.69
$C^{3}C^{7}N^{13}$	116.90
$C^{10}C^{7}N^{13}$	124.77
$C^{7}N^{13}N^{14}$	115.56
$N^{13}N^{14}C^{15}$	123.01
$N^{14}C^{15}S^{17}$	121.06
$N^{16}C^{15}S^{17}$	123.13
dihedral (°)	
$C^{7}N^{13}N^{14}C^{15}$	-86.18
$N^{13}N^{14}C^{15}N^{16}$	16.66
$N^{13}N^{14}C^{15}S^{17}$	-166.21

$C^{15}N^{16}$	1.35
$C^{15}S^{17}$	1.68
Angle (°)	
$C^{2}C^{1}O^{11}$	115.74
$C^{6}C^{1}O^{11}$	124.69
$C^{3}C^{7}N^{13}$	117.73
$C^{10}C^{7}N^{13}$	122.77
$C^{7}N^{13}N^{14}$	119.51
$N^{13}N^{14}C^{15}$	121.98
$N^{14}C^{15}S^{17}$	117.50
$N^{16}C^{15}S^{17}$	129.87
dihedral (°)	
$C^{7}N^{13}N^{14}C^{15}$	-178.57
$N^{13}N^{14}C^{15}N^{16}$	0.58
$N^{13}N^{14}C^{15}S^{17}$	-179.63

The difference between the two molecules is the substitution of on hydrogen in NH_2 group by the aryl radical. So the geometries are difference in this part of the molecules. We notice that the length of $N^{13}N^{14}$ bond is about 1.42 Å in Mol1 and 1.35 Å in Mol2, and some angles are lightly different. The presence of the phenyl group allowed the $C^{7}N^{13}N^{14}C^{15}$chain to be almost flat just like the $N^{13}N^{14}C^{15}S^{17}$ and $N^{13}N^{14}C^{15}N^{16}$ chains.

The electronic surface potential (ESP) of the molecules are showed on figure 2 and 3.The electronic surface potential (ESP) of the molecules are showed on figure 2 and 3.

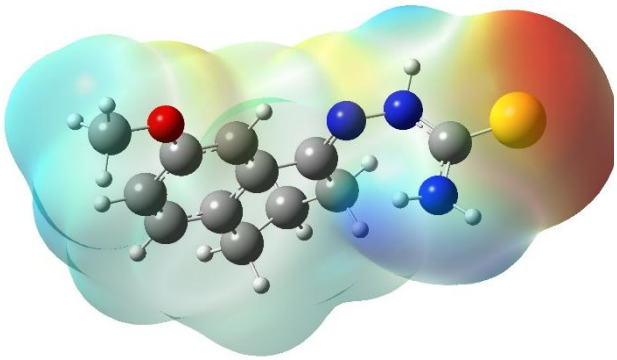

Figure 2 : ESP of Mol1

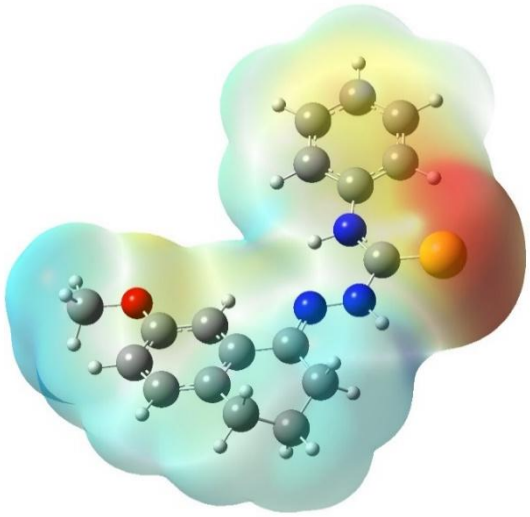

Figure 3 : ESP of Mol2

The red color represents the maximum negative charge density and the blue that of the positive charge. The sulfur atom concentrates the electron density in the two molecules. But in molecule 2 the phenyl group shows also a negative charge density.

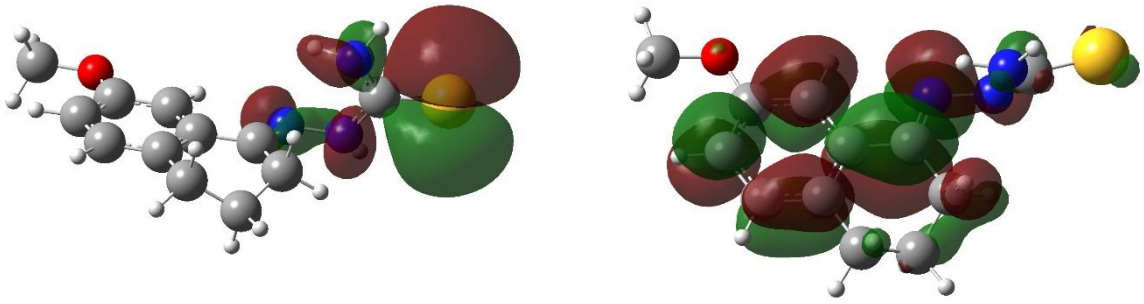

HOMO LUMO

Figure 4 : Orbitales of Mol1

The HOMO orbital which is of type π is almost located on the sulfur atom which will play the donor role in molecule 1. While LUMO is also of type π and involves several atoms of the molecule which can be acceptors of electrons.

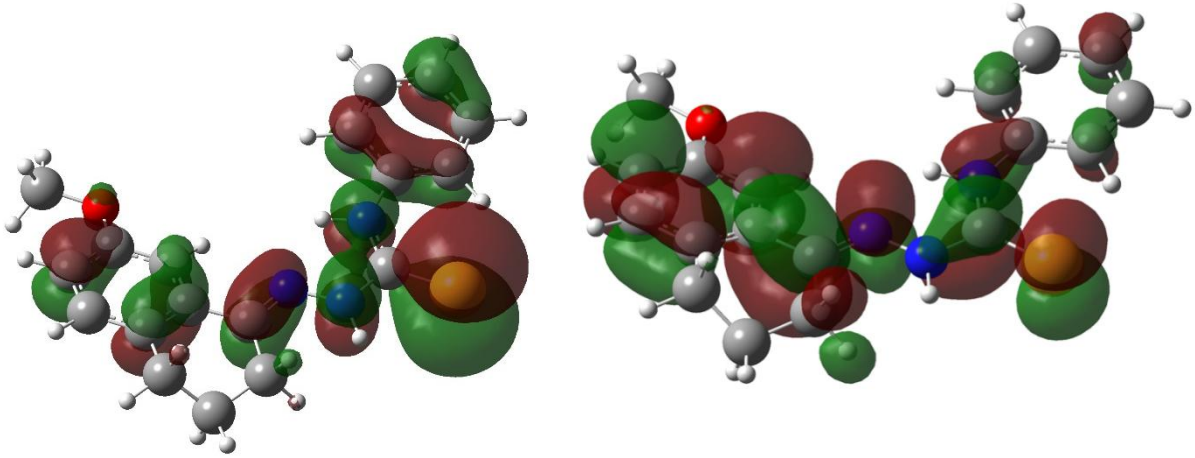

HOMO LUMO

Figure 5 : Orbitales of mol2

In molecule 2, the HOMO is of type π and is distributed over the whole molecule, which could be due to the long conjugation with a strong presence on sulfur. LUMO is also distributed over the entire molecule and is of type π.

The global reactivity indices are given in table 2.

Table 2: Reactivity indices of molecules (DFT/6-31G(d.p) level)

	E_{HOMO}	E_{LUMO}	M	η	ω	ς
Mol1	-0.1978	-0.0605	-0.1292	0.1373	0.0607	7.2833
Mol2	-0.2060	-0.0576	-0.1318	0.1484	0.0585	6.7385

The presence of the phenyl group did not induce a significant change in the calculated reactivity indices. However, we notice a downward shift of the frontier orbitals on the increasing energy axis. The chemical potential of molecule 2 is greater than that of molecule 1, which means that molecule 2 has a greater tendency to gain or lose electrons than molecule 1. The values of electrophilicity and chemical potential show that molecule 2 has a greater tendency to lose electrons.

3.2 ^{1}H-NMR calculation

The tables 3 and 4 show the results of the calculation of ^{1}H-NMR.

Table 3: Calculated ^{1}H-NMR of Mol1

	Exp	6-311G(d,p)	6-311 in DMSO	cc-PVTZ	cc-PVTZ in DMSO
H^{18}	8.05	8.24	8.02	8.31	8.11
H^{19}	7.75	7.25	7.48	7.32	7.55
H^{20}	8.3	6.74	7.05	6.93	7.23

H^{21}	1.7	2.70	2.82	2.81	2.93
H^{22}	1.7	2.85	2.93	2.89	2.96
H^{23}	2.5	1.70	1.73	1.72	1.77
H^{24}	2.5	1.90	1.98	1.96	2.05
H^{25}	2.65	2.18	2.27	2.27	2.37
H^{26}	2.65	3.46	3.28	3.61	3.45
H^{27}	3.8	3.56	3.72	3.64	3.79
H^{28}	3.8	3.57	3.72	3.65	3.79
H^{29}	3.8	4.05	4.1	4.02	4.07
H^{30}	10.09	7.10	7.24	7.46	7.59
H^{31}	6.9	4.28	4.85	4.66	5.21
H^{32}	7.1	4.66	5.06	4.95	5.32

Note that the chemical shifts of hydrogen atoms are well estimated. But the H^{20} and H^{30} atoms show significant differences between the calculated values and the experimental values. Indeed, the H^{30} atom carried by a nitrogen atom is close to another nitrogen atom whose free doublet is available, this hydrogen atom can establish a hydrogen bond which could explain the observed difference. .

For each level of calculation, the correlations between the experimental and theoretical values are as follows:

	Equation	R2
6-311G(d,p)	$\sigma_{exp} = 1.211\sigma_{theo} - 0.302$	0.81
6-311G(d,p) in DMSO	$\sigma_{exp} = 1.233\sigma_{theo} - 0.561$	0.85
cc-PVTZ	$\sigma_{exp} = 1.208\sigma_{theo} - 0.445$	0.84
cc-PVTZ in DMSO	$\sigma_{exp} = 1.222\sigma_{theo} - 0.671$	0.88

The greatest correlation is obtained for the calculation carried out in the cc-PVTZ basis set and in the presence of the solvent.

Table 4: Calculated ^{1}H-NMR of Mol2

	Exp	**6-311G(d.p)**	**6-311G(d.p) in $CDCl_3$**	**cc-PVTZ**	**cc-PVTZ in $CDCl_3$**
H^{27}	2.00	2.68	2.79	2.78	2.86
H^{28}	2.00	2.75	2.78	2.74	2.77
H^{29}	2.65	1.73	1.72	1.75	1.75
H^{30}	2.65	2.05	2.15	2.11	2.18
H^{31}	2.79	2.26	2.44	2.29	2.42
H^{32}	2.79	2.6	2.75	2.72	2.82
H^{33}	3.87	3.64	3.78	3.71	3.8
H^{34}	3.87	3.62	3.75	3.69	3.78
H^{35}	3.87	4.08	4.15	4.05	4.1
H^{36}	9.46	8.02	8.29	8.53	8.7
H^{37}	8.80	9.36	9.65	9.93	10.14

The calculated values correlate with the experimental values in the different calculation levels and with whether or not the solvent is taken into account.

The five hydrogen atoms of the phenyl group have their chemical shifts between 6.92 and 7.78 ppm according to the experimental data, we note that these values are well estimated by the different levels of calculation. Theoretical values are between 6.98-10.12 ppm. The highest chemical shift is that of H^{39}, which is closer to the sulfur atom. The smallest chemical shift is that of the H^{40} atom.

3.3 ^{13}C-NMR calculation

The tables 5 and 6 show the results of the calculation of ^{1}H-NMR.

Table 5: Calculated ^{13}C-NMR of Mol1

	Exp	6-311G(d,p)	6-311G(d,p) in DMSO	cc-PVTZ	cc-PVTZ in DMSO
C^{1}	157.73	165.99	166.29	166.31	166.59
C^{2}	108.3	120.91	119.6	120.5	119.22
C^{3}	132.55	138.49	138.32	139.01	138.82
C^{4}	132.71	140.46	143.18	141.08	143.84
C^{5}	129.45	135.01	136.92	134.96	136.8
C^{6}	116.3	117.05	119.82	117.09	119.74
C^{7}	147.98	184.78	187.65	184.78	187.78
C^{8}	28.11	33.93	34.13	34.03	34.23
C^{9}	25.72	27.28	27.84	27.43	27.99
C^{10}	21.57	31.69	32.73	31.71	32.7
C^{12}	55.27	56.09	57.28	56.19	57.3
C^{15}	178.64	190.98	191.48	192.43	193.21

The calculated chemical shifts of carbon are in agreement with the experimental data in all the calculation levels used. The coefficients of determination are all equal to 0.98. The relationship between the calculated values and the experimental values is given below.

	Equation	R^2
6-311G(d,p)	$\sigma_{exp} = 0.917\sigma_{theo} + 0.299$	0.98
6-311G(d,p) in DMSO	$\sigma_{exp} = 0.912\sigma_{theo} + 0.120$	0.98
cc-PVTZ	$\sigma_{exp} = 0.914\sigma_{theo} + 0.391$	0.98
cc-PVTZ in DMSO	$\sigma_{exp} = 0.908\sigma_{theo} + 0.068$	0.98

Table 6: Calculated ^{13}C-NMR of Mol2

	Exp	6-311G(d.p)	6-311G(d.p) in $CDCl_3$	cc-PVTZ	cc-PVTZ in $CDCl_3$
C^{1}	157.94	166.52	166.87	166.75	167.19
C^{2}	108.60	118.47	118.14	117.82	117.85
C^{3}	131.94	140.35	140.16	141.11	141.18
C^{4}	132.84	138.35	141.48	138.88	141.33
C^{5}	129.52	134.51	136.1	134.47	135.68
C^{6}	116.04	113.74	116.47	113.8	115.81
C^{7}	146.77	145.58	152.08	145.69	150.7
C^{8}	28.23	33.76	34.07	33.72	34.12
C^{9}	25.17	26.42	26.9	26.7	27.18
C^{10}	21.37	28.18	29.13	28.44	29.28
C^{12}	55.19	56.14	57.32	56.22	57.17
C^{15}	175.84	180.09	179.79	181.27	181.49
C^{18}	137.62	146.45	146.98	146.8	147.42
C^{19}	125.87	123.28	125.56	123.11	124.79
C^{20}	125.87	123.0	122.07	122.79	122.43
C^{21}	128.56	133.52	135.75	133.47	135.08
C^{22}	128.56	134.68	135.14	134.75	135.22
C^{23}	123.91	129.1	130.69	128.75	129.88

Taking the solvent into account in the calculations does not significantly modify the results obtained. The estimation of chemical shifts of carbon could be done without taking into account the solvent.

	Equation	R^2
6-311G/gaz	$\sigma_{exp} = 0.988\sigma_{theo} - 2.577$	0.99
6-311/solvent	$\sigma_{exp} = 0.983\sigma_{theo} - 3.292$	0.99
CC-pVTz/gaz	$\sigma_{exp} = 0.985\sigma_{theo} - 2.459$	0.99
CC-pVTz/solvent	$\sigma_{exp} = 0.982\sigma_{theo} - 3.092$	0.99

The calculated values have good relationship with the experimental data, the correlation coefficient is R^2=0.99, for all the calculation level.

4. Conclusion

In the present study, we reported DFT with GIAO calculations of ^{13}C and ^{1}H NMR chemical shifts with respect to TMS, using 6-311G(d,p) and cc-PVTZ basis sets and employing the PCM model to describe solvent effects. The calculation of the chemical shift presents the good correlation with the experimental data. It confirms the structure and the attribution of the chemical shift for each atom. Even if, the calculation in solvent not modify significantly the result in the gas phase, the high correlation was obtained in B3LYP/cc-PVTZ level that take the solvent for calculation of ^{1}H NMR. For the reactivity, the sulfur atom would be the most nucleophilic center of the two molecules.

References

[1]. K. Shivakumar, Shashidhar, P. Vithal Reddy, M. B. Halli, *J. Coord. Chem.* 2008, *61*, 2274.
[2]. M. T. H. Tarafder, M. A. Ali, D. J. Wee, K. Azahari, S. Silong, K. A. Crouse, *Transit. Met. Chem.* 2000, *25*, 456.
[3]. N. Dharmaraj, P. Viswanathamurthi, K. Natarajan, *Transit. Met. Chem.* 2001, *26*, 105.
[4]. A. L. R. Sales, J. M. Silla, J. L. Neto, C. P. A. Anconi, *J. Mol. Model.* 2021, *27*.
[5]. M. Kaushal, T. S. Lobana, L. Nim, J. Kaur, R. Bala, G. Hundal, et al., *New J. Chem.* 2018, *42*, 15879.
[6]. D. Rogolino, A. Bacchi, L. De Luca, G. Rispoli, M. Sechi, A. Stevaert, et al., *JBIC J. Biol. Inorg. Chem.* 2015, *20*, 1109.
[7]. S. Umamatheswari, S. Kabilan, *J. Enzyme Inhib. Med. Chem.* 2011, *26*, 430.
[8]. C. Zani, F. Bisceglie, F. M. Restivo, D. Feretti, M. Pioli, F. Degola, et al., *Food Chem. Toxicol.* 2017, *105*, 498.
[9]. H. Beraldo, *Quím. Nova* 2004, *27*, 461.
[10]. J. P. Mallari, A. Shelat, A. Kosinski, C. R. Caffrey, M. Connelly, F. Zhu, et al., *Bioorg. Med. Chem. Lett.* 2008, *18*, 2883.
[11]. E. M. Jouad, A. Riou, M. Allain, M. A. Khan, G. M. Bouet, *Polyhedron* 2001, *20*, 67.
[12]. D. C. Greenbaum, Z. Mackey, E. Hansell, P. Doyle, J. Gut, C. R. Caffrey, et al., *J. Med. Chem.* 2004, *47*, 3212.
[13]. S. F. Sousa, G. R. P. Pinto, A. J. M. Ribeiro, J. T. S. Coimbra, P. A. Fernandes, M. J. Ramos, *J. Comput. Chem.* 2013, *34*, 2079.
[14]. H. B. Schlegel, *WIREs Comput. Mol. Sci.* 2011, *1*, 790.
[15]. M. Marín-Luna, R. M. Claramunt, C. López, M. Pérez-Torralba, D. Sanz, F. Reviriego, et al., *Solid State Nucl. Magn. Reson.* 2020, *108*, 101676.
[16]. I. Alkorta, J. Elguero, C. Dardonville, F. Reviriego, D. Santa María, R. M. Claramunt, et al., *J. Phys. Org. Chem.* 2020, *33*.
[17]. W. Holzer, L. Castoldi, V. Kyselova, D. Sanz, R. M. Claramunt, M. C. Torralba, et al., *Struct. Chem.* 2019, *30*, 1729.
[18]. A. Bagno, F. Rastrelli, G. Saielli, *J. Phys. Chem. A*2003, *107*, 9964.
[19]. H. C. Da Silva, W. B. De Almeida, *Chem. Phys.* 2020, *528*, 110479.
[20]. A. Gryff-Keller, *Concepts Magn. Reson. Part A*2011, *38A*, 289.
[21]. H. Chermette, *J. Comput. Chem.* 1999, *20*, 129.

[22]. K. Fukui, In *Theory of Orientation and Stereoselection*, Fukui, K., Ed., Springer Berlin Heidelberg, Berlin, Heidelberg, 1975, pp. 34–39.
[23]. D. Glossman-Mitnik, *2013 Int. Conf. Comput. Sci.* 2013, *18*, 816.
[24]. A. J. Cohen, P. Mori-Sánchez, W. Yang, *Chem. Rev.* 2012, *112*, 289.
[25]. E. Engel, R. M. Dreizler, In *Density Functional Theory: An Advanced Course*, Engel, E., Dreizler, R. M., Eds., Springer Berlin Heidelberg, Berlin, Heidelberg, 2011, pp. 11–56.
[26]. A. D. Becke, *J. Chem. Phys.* 1993, *98*, 5648.
[27]. B. Mennucci, E. Cancès, J. Tomasi, *J. Phys. Chem. B*1997, *101*, 10506.
[28]. K. Wolinski, J. F. Hinton, P. Pulay, *J. Am. Chem. Soc.* 1990, *112*, 8251.
[29]. M. J. Frisch, G. W. Trucks, H. B. Schlegel, G. E. Scuseria, M. A. Robb, J. R. Cheeseman, G. Scalmani, V. Barone, B. Mennucci, G. A. Petersson, H. Nakatsuji, M. Caricato, X. Li, H. P. Hratchian, A. F. Izmaylov, J. Bloino, G. Zheng, J. L. Sonnenberg, M. Hada, M. Ehara, K. Toyota, R. Fukuda, J. Hasegawa, M. Ishida, T. Nakajima, Y. Honda, O. Kitao, H. Nakai, T. Vreven, J. A. Montgomery, Jr., J. E. Peralta, F. Ogliaro, M. Bearpark, J. J. Heyd, E. Brothers, K. N. Kudin, V. N. Staroverov, R. Kobayashi, J. Normand, K. Raghavachari, A. Rendell, J. C. Burant, S. S. Iyengar, J. Tomasi, M. Cossi, N. Rega, J. M. Millam, M. Klene, J. E. Knox, J. B. Cross, V. Bakken, C. Adamo, J. Jaramillo, R. Gomperts, R. E. Stratmann, O. Yazyev, A. J. Austin, R. Cammi, C. Pomelli, J. W. Ochterski, R. L. Martin, K. Morokuma, V. G. Zakrzewski, G. A. Voth, P. Salvador, J. J. Dannenberg, S. Dapprich, A. D. Daniels, Ö. Farkas, J. B. Foresman, J. V. Ortiz, J. Cioslowski, and D. J. Fox, Gaussian 09 (Gaussian, Inc., Wallingford CT, 2009).